MG132 or ALLN, and lactacystin are widely used proteasome inhibitors. However, peptide aldehydes also inhibit cathepsins and calpains, and lactacystin inhibits cathepsin A (21, 22). Because these inhibitors are not proteasome-specific and may interfere with lysosomal function, we used epoxomicin as a selective proteasome inhibitor (23, 24). We observed protein clearance of human SOD1 in Neuro2a cells transfected with mutant or wild-type SOD1 in the presence of the translation inhibitor cycloheximide (Fig. 1*A*, *i* and *ii*). Consistent with previous reports (9, 11), wild-type SOD1 exhibited a relatively long half-life (half-life of more than 24 h) compared with mutant SOD1 (~10 h; G93A) (Fig. 1*A*, *iii*). The degradation of wild-type and mutant SOD1 was suppressed by epoxomicin treatment (Fig. 1, *B* and *C*) (~14-h increase in half-life; G93A; Fig. 1*A*, *ii*). Our finding that mutant SOD1 is degraded by the proteasome is in agreement with previous reports (8, 9). To determine whether endogenous human wild-type SOD1 is also degraded by the proteasome, SOD1 clearance was examined using the human neuroblastoma SH-SY5Y cell line. The proteasome inhibitor treatment promoted the accumulation of human SOD1 proteins (Fig. 1, *D* and *E*). These results indicate that endogenous wild-type SOD1 is degraded by the proteasome, also consistent with a previous report (14).

Wild-type and Mutant SOD1 Are Also Degraded by Macroautophagy—To date, there have been no reports of macroautophagy participating in human SOD1 clearance. We therefore investigated whether wild-type or mutant SOD1 was degraded by macroautophagy using 3-MA, an inhibitor of macroautophagy (18, 25, 26), and ammonium chloride, an inhibitor of lysosomal proteolysis (26). We initially confirmed that 3-MA inhibits the formation of autophagosomes in Neuro2a cells using green fluorescent protein-LC3, a marker of autophagosomes (27) (supplemental Fig. S2). Moreover, we also showed that the clearance of α-synuclein, an established substrate for macroautophagy (28), was inhibited by 3-MA or ammonium chloride treatment (supplemental Fig. S3). Treatment of Neuro2a cells with 3-MA promoted the accumulation of G93A mutant SOD1 proteins (Fig. 2*A*). In the presence of cycloheximide, the degradation of wild-type and mutant SOD1 was suppressed by treatment with 3-MA (Fig. 2, *B* and *C*) (a more than 14-h increase in half-life; G93A, Fig. 2*B*), indicating that wild-type and mutant SOD1 are degraded by macroautophagy in these cells and that the accumulation of SOD1 proteins by 3-MA is not due to increased protein synthesis. These results, together with Fig. 1, suggest that mutant SOD1 are degraded more rapidly than wild-type SOD1 by macroautophagy (it is estimated that 15–20% of wild-type SOD1 and 25–30% of mutant SOD1 were degraded by macroautophagy during the 24-h incubation). The clearance of mutant G93A SOD1 was also decreased by treatment with ammonium chloride (Fig. 2*D*). As shown in Supplemental Fig. S4 and Fig. 2*D*, the protein level of endogenous mouse SOD1 was increased by 3-MA or ammonium chloride treatment. The result shown in Fig. 2*D* further supports the role of the lysosomes in SOD1 degradation. To test the role of macroautophagy on SOD1 degradation in differentiated neuronal cells or neurons, we also used differentiated Neuro2a cells. In differentiated Neuro2a cells, 3-MA increased both wild-type and mutant SOD1 protein levels in the presence or absence of

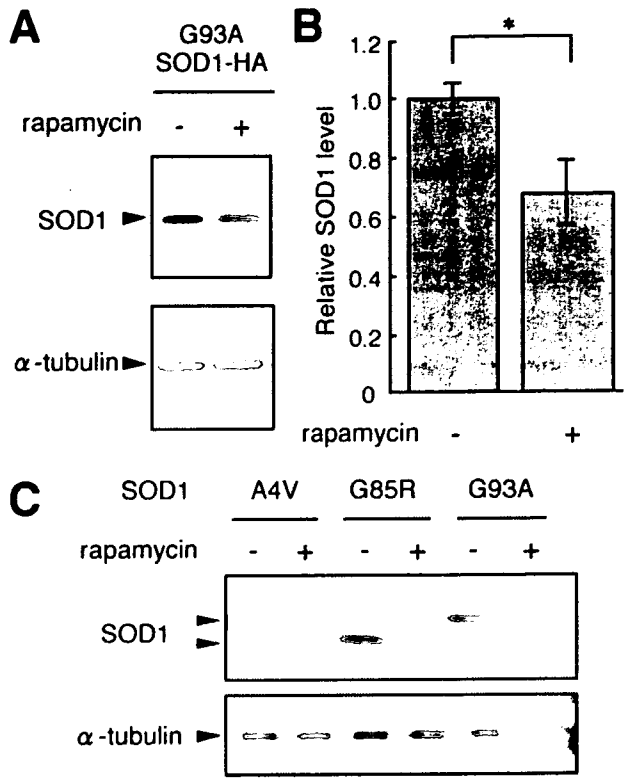

FIGURE 3. **Rapamycin treatment decreases mutant SOD1 protein levels.** *A* and *B*, Neuro2a cells were transiently transfected with HA-tagged G93A SOD1. 24 h after transfection, cells were incubated with or without 100 nM rapamycin for 24 h. Total cell lysates were analyzed by immunoblotting using anti-SOD1 antibody. α-Tubulin was used as a loading control (*A*). The relative level of mutant G93A SOD1 was quantified by densitometry. Data are presented as the means ± S.E. ($n = 3$). *, $p < 0.05$ (*B*). *C*, Neuro2a cells transfected with mutant A4V, G85R, or G93A SOD1 were cultured in differentiation medium with or without 200 nM rapamycin for 24 h. Total cell lysates were analyzed by immunoblotting.

cycloheximide (data not shown). To determine whether endogenous human SOD1 is degraded by macroautophagy, the clearance of endogenous SOD1 was examined in SH-SY5Y cells. As shown in Fig. 2, *E* and *F*, the degradation of endogenous SOD1 proteins was inhibited by 3-MA.

For further confirmation of the clearance of SOD1 by macroautophagy, we used rapamycin to induce macroautophagy (29, 30), and gene silencing with siRNA to inhibit macroautophagy. Treating Neuro2a cells with rapamycin decreased HA-tagged G93A SOD1 levels (Fig. 3, *A* and *B*). In differentiated Neuro2a cells, SOD1 protein levels were also decreased by rapamycin (Fig. 3*C*). Beclin 1 is a component of a class III phosphatidylinositol 3-kinase complex that is crucial for macroautophagy (31). Silencing of the Beclin 1 gene by siRNA inhibits the generation of autophagosomes, thus preventing macroautophagy (32). Atg7 protein is also essential for macroautophagy (17). We initially confirmed that Beclin 1 or Atg7 expression was knocked down by Beclin 1 or Atg7 siRNA, respectively (Fig. 4, *A* and *B*). We also showed that α-synuclein level was increased by Beclin 1 or Atg7 siRNA (supplemental Fig. S3). We observed inhibited degradation of wild-type and mutant SOD1 in cells with Beclin 1 siRNA (Fig. 4, *A* and *C*) or Atg7 siRNA (Fig. 4, *B* and *D*) compared with cells with control siRNA (~14 h increase in half-life; G93A; Fig. 4*E*). The results shown in Figs. 2–4 demonstrate that wild-type and mutant SOD1 are also

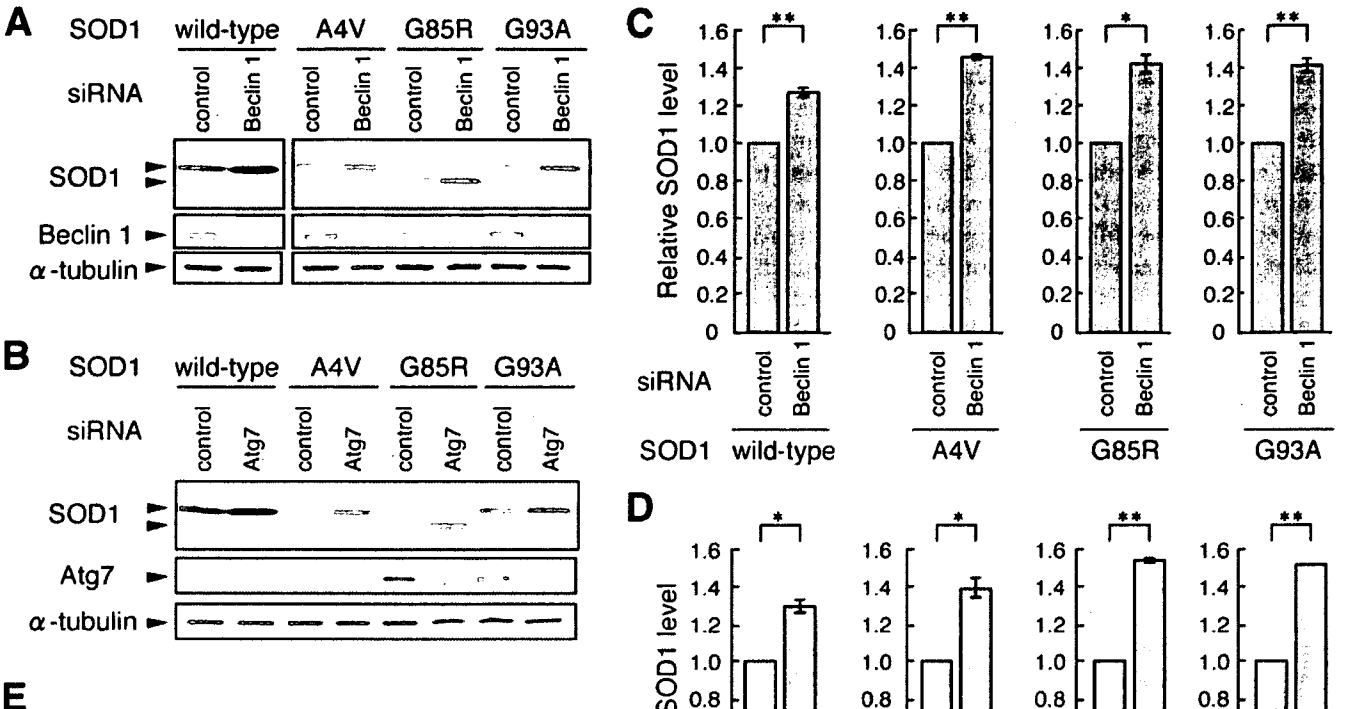

FIGURE 4. **Silencing of macroautophagy genes promote the accumulation of SOD1 proteins.** *A* and *C*, Neuro2a cells were cotransfected with SOD1 (wild-type, A4V, G85R, or G93A) and siRNA (Beclin 1 siRNA or control EGFP siRNA). 24 h after transfection, total cell lysates were prepared and analyzed by immunoblotting using anti-SOD1 or anti-Beclin 1 antibody. α-Tubulin was used as a control (*A*). Levels of SOD1 were quantified by densitometry, and the levels are expressed as -fold level of SOD1 in cells with Beclin 1 siRNA over cells with control siRNA. Data are presented as the means ± S.E. ($n = 3$). *, $p < 0.05$; **, $p < 0.01$ (*C*). *B* and *D*, Neuro2a cells were cotransfected with SOD1 (wild-type, A4V, G85R, or G93A) and siRNA (Atg7 siRNA or control siRNA). 24 h after transfection, total cell lysates were prepared and analyzed by immunoblotting using anti-SOD1, anti-Atg7, or anti-α-tubulin antibody (*B*). Levels of SOD1 were quantified by densitometry, and the levels are expressed as -fold level of SOD1 in cells with Atg7 siRNA over cells with control siRNA. Data are presented as the means ± S.E. ($n = 3$). *, $p < 0.05$; **, $p < 0.01$ (*D*). *E*, Neuro2a cells cotransfected with G93A SOD1 and siRNA (control, Atg7, or Beclin 1 siRNA) were treated with 10 μg/ml cycloheximide for the indicated time and lysed. Total cell lysates were analyzed by immunoblotting using anti-SOD1 or anti-α-tubulin antibody.

degraded by macroautophagy in neuronal cells. In the nonneuronal COS-7 cells, ammonium chloride or 3-MA treatment stimulated the accumulation of HA-tagged wild-type SOD1 and G93A SOD1 (Fig. 5*A*) or mutant G93A SOD1 (Fig. 5*B*), respectively. Treatment of the cells with epoxomicin also increased wild-type and mutant SOD1 levels (Fig. 5*C* and supplemental Fig. S5). These results indicate that wild-type and mutant SOD1 are degraded by both macroautophagy and the proteasome in COS-7 cells. The results shown in Figs. 3*A* and 5*A* indicate that not only SOD1 without a tag but also HA-tagged SOD1 is degraded by macroautophagy.

The Contributions of the Proteasome Pathway and Macroautophagy to Mutant SOD1 Degradation Are Comparable—We then assessed the relative contributions of proteasomal degradation and macroautophagy to the clearance of mutant SOD1. As shown in Fig. 6*A*, 10 mM 3-MA entirely suppresses the (3-MA-sensitive) macroautophagy-mediated degradation of mutant SOD1. 1 μM epoxomicin also entirely suppresses the (epoxomicin-sensitive) proteasome-mediated degradation of mutant SOD1 (Fig. 6*B* and supplemental Fig. S6). Therefore, we compared mutant G93A SOD1 levels in 1 μM epoxomicin-treated cells with that of 10 mM 3-MA-treated cells. The SOD1 protein level in 3-MA-treated cells was comparable with that of epoxomicin-treated cells (Fig. 6, *C–F*). An increased accumulation of mutant SOD1 was detected in cells cotreated with both inhibitors compared with that of 3-MA-treated cells or epoxomicin-treated cells (Fig. 6, *E* and *F*). These data further support the idea that mutant SOD1 proteins are degraded by both macroautophagy and the proteasome and indicate that, in these cells, the contribution of macroautophagy to mutant SOD1 clearance is approximately equal to that of the proteasome pathway.

Macroautophagy Reduces the Toxicity of Mutant SOD1—Previous studies have shown that mutant SOD1-expressing cells are more susceptible to cell death induced by proteasome inhibition (33). We examined whether inhibiting the macroautophagy-mediated degradation of mutant SOD1 could also induce cell death in Neuro2a cells using three different assays.

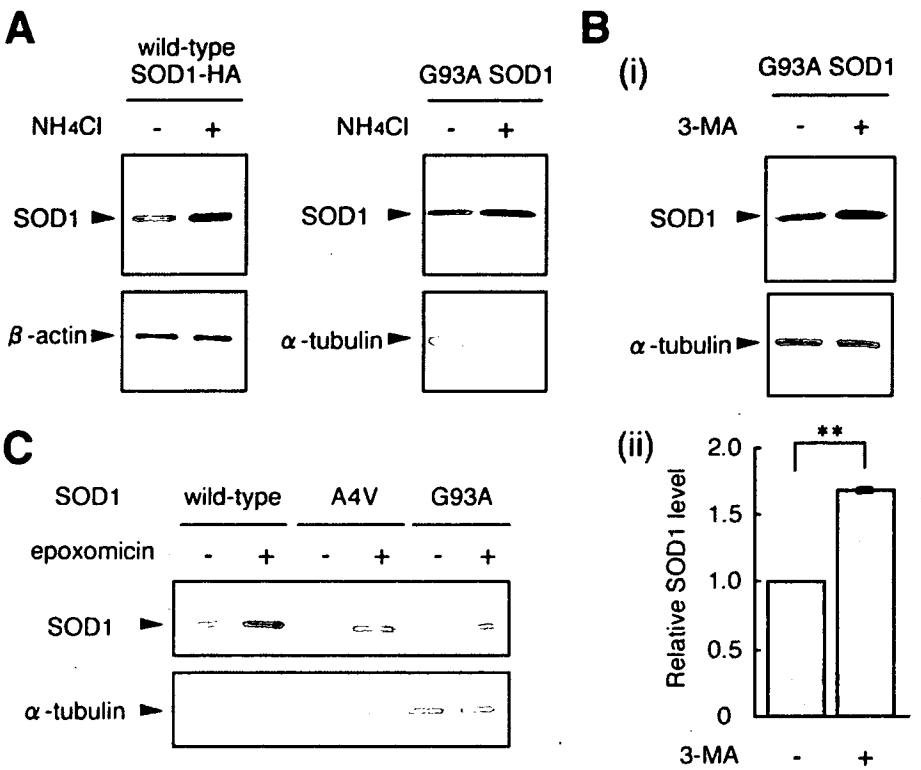

FIGURE 5. **Mutant and wild-type SOD1 are degraded by both macroautophagy and the proteasome in COS-7 cells.** *A*, COS-7 cells were transiently transfected with HA-tagged human wild-type SOD1 or G93A SOD1. 24 h after transfection, cells were incubated with or without 20 mM NH_4Cl for 24 h. Total cell lysates were analyzed by immunoblotting using anti-HA antibody or anti-SOD1 antibody. β-Actin and α-tubulin were used as loading controls. *B*, COS-7 cells transfected with G93A mutant SOD1 were incubated with or without 10 mM 3-MA in the presence of cycloheximide for 24 h. Total cell lysates were analyzed by immunoblotting using anti-SOD1 antibody (*i*). Levels of SOD1 were quantified by densitometry, and the levels are expressed as -fold level of SOD1 in cells with 3-MA over control. Data are presented as the means ± S.E. ($n = 3$). **, $p < 0.01$ (*ii*). *C*, COS-7 cells were transfected with wild-type or mutant A4V or G93A SOD1. 24 h after transfection, cells were incubated with or without 10 nM epoxomicin for 24 h. Total cell lysates were analyzed by immunoblotting.

nonionic detergent-soluble and -insoluble SOD1. The nonionic detergent-soluble and -insoluble fractions were subjected to SDS-PAGE following Western blotting. In agreement with a previous report (9), mutant SOD1 proteins exhibited increased nonionic detergent insolubility compared with wild-type SOD1 (Fig. 8*B*). The increased level of wild-type SOD1 compared with mutant in the detergent-soluble fraction (Fig. 8*A*) is probably due to the rapid turnover of mutant SOD1. Incubation with 3-MA increased monomer SOD1 levels in the detergent-soluble (Fig. 8*A*) and -insoluble fractions (Fig. 8*B*), suggesting that both detergent-soluble and -insoluble SOD1 are degraded by macroautophagy. Consistent with a previous report (9), we found SDS-resistant dimers and high molecular weight aggregates of mutant SOD1 in the detergent-insoluble fraction (Fig. 8*C*). These dimers and aggregates of mutant SOD1 were increased by 3-MA treatment (Fig. 8*C*), suggesting that insoluble aggregates of mutant SOD1 are also cleared by macroautophagy. The results from Figs. 7 and 8 indicate that the accumulation of toxic mutant SOD1 proteins by macroautophagy inhibition leads to greater cell death.

For assessment of cell viability, we used the MTS assay and ATP assay, and for assessment of cell death, we used the lactate dehydrogenase release assay. In untreated differentiated Neuro2a cells, there was no statistically significant difference in cell viability or cell death among control cells, wild-type SOD1-expressing cells, and mutant SOD1-expressing cells (Fig. 7, *A–C*). However, when cells were treated with 3-MA, mutant SOD1-expressing cells showed significantly increased cell death and significantly decreased cell viability compared with control cells or wild-type SOD1-expressing cells (Fig. 7, *D–F*). When compared with cell death of 3-MA-untreated cells, cell death of 3-MA-treated cells was increased in mutant SOD1-expressed cells but not in cells with wild-type SOD1 (Fig. 7*G*). From these results, we conclude that macroautophagy reduces mutant SOD1-mediated toxicity in this cell model.

Inhibition of Macroautophagy Leads to Accumulation of both Detergent-soluble and Detergent-insoluble Mutant SOD1—Detergent-insoluble SOD1 proteins, aggregates, or inclusion bodies have been found in motor neurons in fALS patients (34), mouse models of fALS (35), and the cells transfected with mutant SOD1 (9, 36), although it is not clear whether these insoluble SOD1 proteins and aggregates are toxic because of conflicting results on the correlation between aggregate formation and cell death (36, 37). We investigated the effect of macroautophagy inhibition on the clearance of

DISCUSSION

Using inhibitors of macroautophagy and proteasomal degradation, we have shown that both wild-type and mutant SOD1 proteins are degraded by both pathways. Accumulating evidence has shown that mutant SOD1 is degraded by the ubiquitin-proteasome pathway (8, 9, 19). However, most of these studies have used lactacystin or a peptide aldehyde, both of which are not proteasome-specific inhibitors. Our data on the effect of the selective proteasome inhibitor epoxomicin also indicate that mutant SOD1 is degraded by the proteasome. Because wild-type SOD1 is not ubiquitinated by the ubiquitin ligases (10, 11), it has been proposed that wild-type SOD1 is not a substrate of the proteasome. However, a recent report has suggested that wild-type SOD1 can be degraded by the 20 S proteasome without ubiquitination (14). Moreover, we show here that epoxomicin treatment increases both overexpressed and endogenous wild-type SOD1 levels. Our data together with the previous reports support the idea that wild-type SOD1 is degraded by the 20 S proteasome in mammalian cells.

In this study, we demonstrated for the first time that macro-

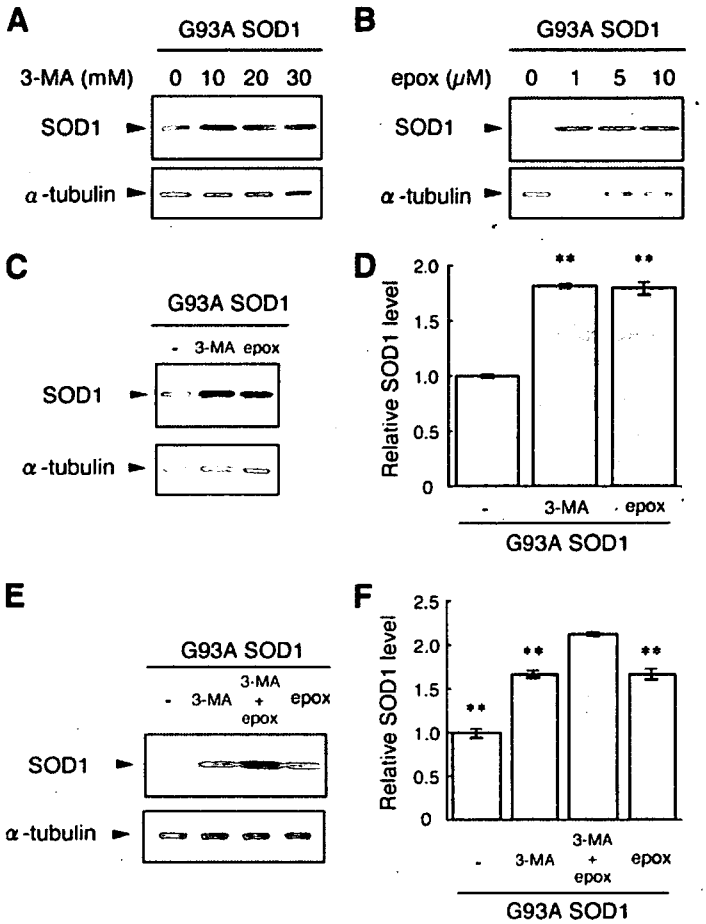

FIGURE 6. **The contribution of macroautophagy to SOD1 clearance is comparable with that of the proteasome.** *A*, Neuro2a cells transfected with mutant G93A SOD1 were incubated with or without 10, 20, or 30 mM 3-MA for 24 h. Total cell lysates were analyzed by immunoblotting. *B*, Neuro2a cells transfected with mutant G93A SOD1 were incubated with or without 1, 5, or 10 μM epoxomicin (*epox*) for 24 h. Total cell lysates were analyzed by immunoblotting. *C* and *D*, Neuro2a cells transfected with mutant G93A SOD1 were incubated with or without 10 mM 3-MA or 1 μM epoxomicin for 24 h. Total cell lysates were analyzed by immunoblotting (*C*). The relative level of mutant G93A SOD1 was quantified by densitometry. Data are presented as the means ± S.E. ($n = 3$). **, $p < 0.01$ in comparison with control (analysis of variance with Dunnett's multiple comparison test). (*D*). *E* and *F*, COS-7 cells transfected with mutant G93A SOD1 were incubated with or without 10 mM 3-MA, 1 μM epoxomicin, or both inhibitors (10 mM 3-MA and 1 μM epoxomicin) in the presence of cycloheximide for 24 h. Total cell lysates were analyzed by immunoblotting (*E*). The relative level of mutant G93A SOD1 was quantified by densitometry. Data are presented as the means ± S.E. ($n = 3$). **, $p < 0.01$ in comparison with 3-MA + epoxomicin (analysis of variance with Dunnett's multiple comparison test) (*F*).

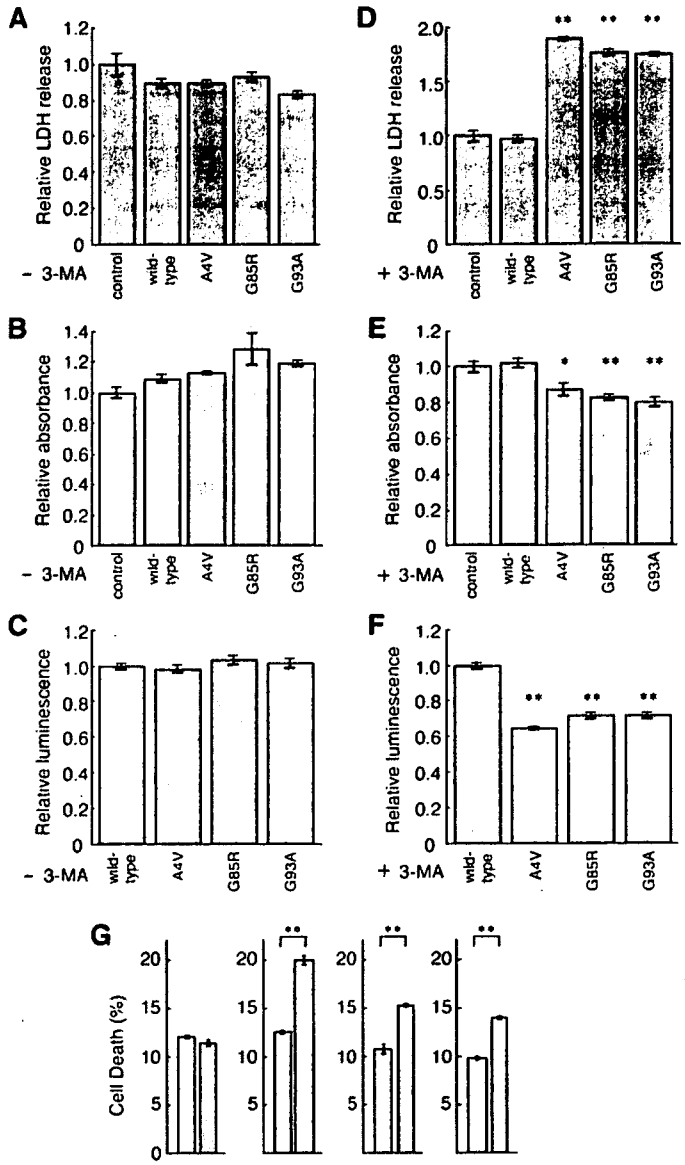

FIGURE 7. **Macroautophagy inhibition causes mutant SOD1-mediated cell death.** *A–G*, Neuro2a cells were transiently transfected with control empty vector (*A*, *B*, *D*, and *E*) or human SOD1 (wild type, A4V, G85R, or G93A). 24 h after transfection, cells were incubated in differentiation medium with (*D–G*) or without (*A–C* and *G*) 10 mM 3-MA for 24 h, and the lactate dehydrogenase release assay (*A*, *D*, and *G*), MTS assay (*B* and *E*), or ATP assay (*C* and *F*) were performed. The percentage of nonviable cells in each sample was calculated from the lactate dehydrogenase release assay (*G*). The experiment in *G* was performed independently of *A* and *D*. Data are expressed as the means ± S.E. ($n = 4$ in *A*, *C*, *D*, *F*, and *G*; $n = 3$ in *B* and *E*). *, $p < 0.05$; **, $p < 0.01$ in comparison with control (*A*, *B*, *D*, and *E*) or with wild-type SOD1 (*C* and *F*) (analysis of variance with Dunnett's multiple comparison test). **, $p < 0.01$ (*G*; *t* test).

autophagy is another pathway for degradation of wild-type and mutant SOD1. Our findings are consistent with a previous report that rat wild-type SOD1 is present in autophagosomes and lysosomes in rat hepatocytes (although they did not examine whether rat SOD1 was degraded by macroautophagy in those cells) (38). We propose that the contribution of macroautophagy to mutant SOD1 degradation is comparable with that of the proteasome pathway in the cell types we tested. Recent studies have demonstrated that transgenic mice with neuron-specific expression of mutant SOD1 do not exhibit an ALS-like phenotype (39, 40) and that neurodegeneration is delayed when motor neurons expressing mutant SOD1 are surrounded by healthy nonneuronal wild-type cells (41). In addition, Urushitani *et al.* (42) have shown that chromogranins promote secretion of mutant SOD1 from cells expressing the mutant protein, and they proposed that secreted mutant SOD1 can be toxic to neighboring cells. These studies strongly suggest that the expression of mutant SOD1 in nonneuronal cells may be involved in mutant SOD1-mediated neurotoxicity. In nonneuronal COS-7 cells, mutant SOD1 is also degraded by both the proteasome and macroautophagy (Fig. 5). Thus, not only the proteasome but also macroautophagy may play an important

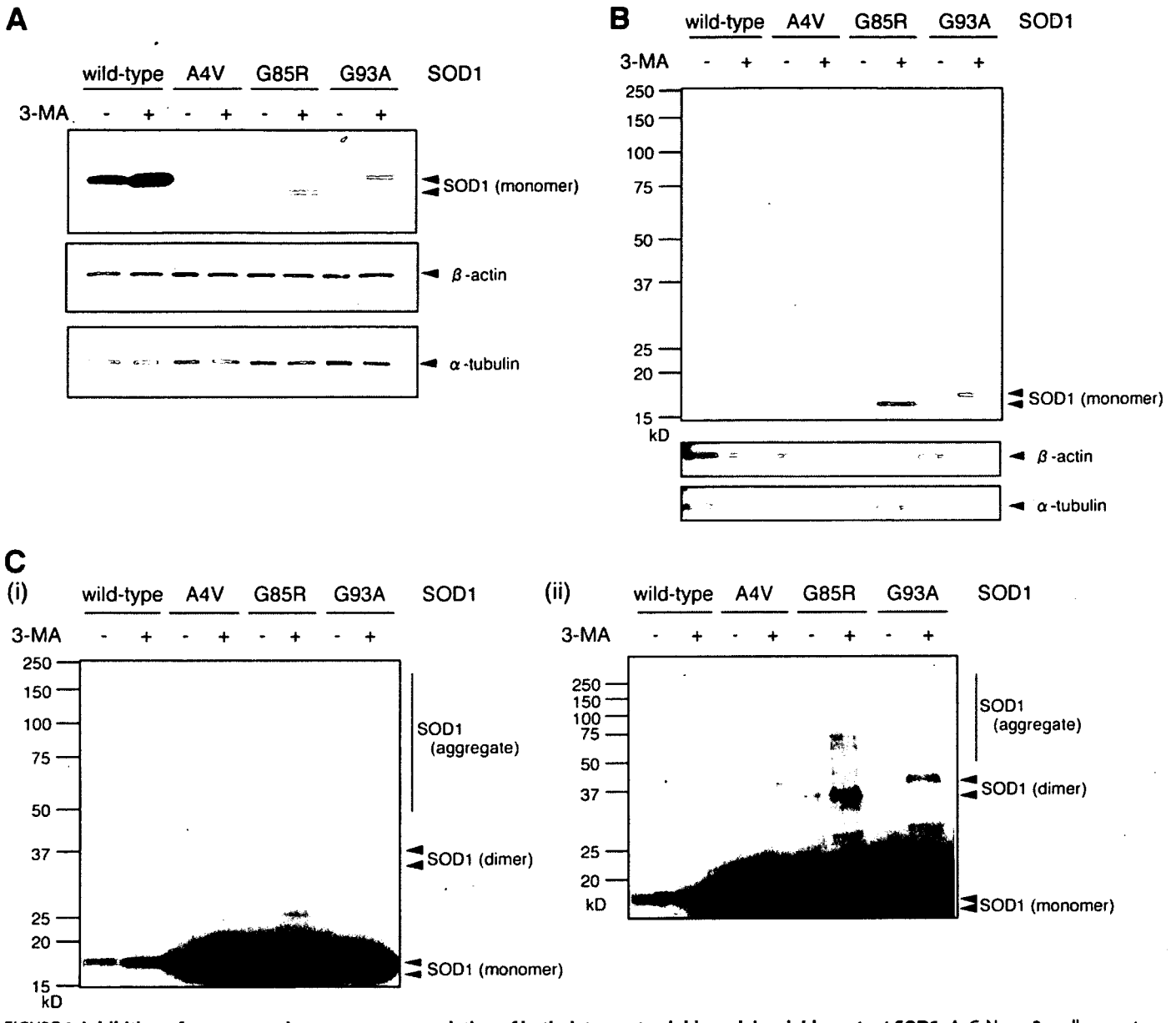

FIGURE 8. **Inhibition of macroautophagy causes accumulation of both detergent-soluble and -insoluble mutant SOD1.** *A–C*, Neuro2a cells were transiently transfected with human wild-type or mutant A4V, G85R, or G93A SOD1. 24 h after transfection, cells were cultured in differentiation medium with or without 10 mM 3-MA for 24 h. Triton X-100-soluble (*A*) and -insoluble (*B* and *C*) fractions were prepared and analyzed by immunoblotting using anti-SOD1 antibody. β-Actin and α-tubulin were used as loading controls. *C* (*i*), a longer exposure of *B*. *C* (*i* and *ii*), two different sets of experiments with longer exposure.

role in clearance of mutant SOD1 in fALS in nonneuronal cells as well as in neuronal cells.

It has been well established that mutant SOD1-mediated toxicity is caused by a gain of toxic function rather than the loss of SOD1 activity (1, 2). The appearance of mutant SOD1 aggregates in motor neurons in fALS patients and mouse models of fALS (34, 35) has suggested that aggregation has a role in neurotoxicity. However, conflicting results have been reported on the correlation between aggregate formation and cell death. A recent study has shown that the ability of mutant G85R and G93A SOD1 proteins to form aggregates correlates with neuronal cell death using live cell imaging techniques (36). Another report has concluded that aggregate formation of A4V and V148G SOD1 mutants does not correlate with cell death (37). These controversies also exist in other neurodegenerative diseases (43–46). Our current data suggest that macroautophagy degrades toxic species of mutant SOD1 and that the accumulation of mutant SOD1 proteins leads to greater cell death. However, whether the toxic SOD1 species are monomers, oligomers, or aggregates cannot be determined from our study, because a variety of mutant SOD1 species, including detergent-soluble SOD1 monomers and detergent-insoluble monomers, dimers, and aggregates, were accumulated by macroautophagy inhibition (Fig. 8).

Our data show that macroautophagy reduces mutant SOD1-mediated toxicity and that induction of macroautophagy decreases mutant SOD1 protein levels. Niwa *et al.* (10) have shown that the ubiquitin ligase Dorfin ubiquitinates mutant SOD1 and prevents the neurotoxicity of mutant SOD1. Taken together, these data imply that macroautophagy inducers, acti-

vators of the ubiquitin-proteasome pathway, or a combination of the two have therapeutic potential for fALS. In conclusion, our results demonstrate that mutant SOD1 is degraded by at least two pathways, macroautophagy and the proteasome pathway, and that the clearance of mutant SOD1 by macroautophagy reduces its cell toxicity. These findings may provide insight into the molecular mechanisms of the pathogenesis of fALS.

Acknowledgments—We thank Dr. Ryosuke Takahashi (Kyoto University) and Dr. Makoto Urushitani (Laval University) for the gift of pcDNA3-hSOD1 (wild-type and mutant A4V, G85R, and G93A) plasmids, and Naoki Takagaki for the support in English.

REFERENCES

1. Bruijn, L. I., Miller, T. M., and Cleveland, D. W. (2004) *Annu. Rev. Neurosci.* **27**, 723–749
2. Cleveland, D. W., and Rothstein, J. D. (2001) *Nat. Rev. Neurosci.* **2**, 806–819
3. Rosen, D. R., Siddique, T., Patterson, D., Figlewicz, D. A., Sapp, P., Hentati, A., Donaldson, D., Goto, J., O'Regan, J. P., Deng, H. X., Rahmani, Z., Krizus, A., McKenna-Yasek, D., Cayabyab, A., Gaston, S. M., Berger, R., Tanzi, R. E., Halperin, J. J., Herzfeldt, B., Van den Bergh, R., Hung, W. Y., Bird, T., Deng, G., Mulder, D. W., Smyth, C., Laing, N. G., Soriano, E., Pericak-Vance, M. A., Haines, J., Rouleau, G. A., Gusella, J. S., Horvitz, H. R., and Brown, R. H., Jr. (1993) *Nature* **362**, 59–62
4. Gurney, M. E., Pu, H., Chiu, A. Y., Dal Canto, M. C., Polchow, C. Y., Alexander, D. D., Caliendo, J., Hentati, A., Kwon, Y. W., Deng, H. X., Chen, W., Zhai, P., Sufit, R. L., and Siddique, T. (1994) *Science* **264**, 1772–1775
5. Reaume, A. G., Elliott, J. L., Hoffman, E. K., Kowall, N. W., Ferrante, R. J., Siwek, D. F., Wilcox, H. M., Flood, D. G., Beal, M. F., Brown, R. H., Jr., Scott, R. W., and Snider, W. D. (1996) *Nat. Genet.* **13**, 43–47
6. Goldberg, A. L. (2003) *Nature* **426**, 895–899
7. Cuervo, A. M. (2004) *Trends Cell Biol.* **14**, 70–77
8. Hoffman, E. K., Wilcox, H. M., Scott, R. W., and Siman, R. (1996) *J. Neurol. Sci.* **139**, 15–20
9. Johnston, J. A., Dalton, M. J., Gurney, M. E., and Kopito, R. R. (2000) *Proc. Natl. Acad. Sci. U. S. A.* **97**, 12571–12576
10. Niwa, J., Ishigaki, S., Hishikawa, N., Yamamoto, M., Doyu, M., Murata, S., Tanaka, K., Taniguchi, N., and Sobue, G. (2002) *J. Biol. Chem.* **277**, 36793–36798
11. Miyazaki, K., Fujita, T., Ozaki, T., Kato, C., Kurose, Y., Sakamoto, M., Kato, S., Goto, T., Itoyama, Y., Aoki, M., and Nakagawara, A. (2004) *J. Biol. Chem.* **279**, 11327–11335
12. Shringarpure, R., Grune, T., Mehlhase, J., and Davies, K. J. (2003) *J. Biol. Chem.* **278**, 311–318
13. Asher, G., Tsvetkov, P., Kahana, C., and Shaul, Y. (2005) *Genes Dev.* **19**, 316–321
14. Di Noto, L., Whitson, L. J., Cao, X., Hart, P. J., and Levine, R. L. (2005) *J. Biol. Chem.* **280**, 39907–39913
15. Komatsu, M., Waguri, S., Chiba, T., Murata, S., Iwata, J., Tanida, I., Ueno, T., Koike, M., Uchiyama, Y., Kominami, E., and Tanaka, K. (2006) *Nature* **441**, 880–884
16. Hara, T., Nakamura, K., Matsui, M., Yamamoto, A., Nakahara, Y., Suzuki-Migishima, R., Yokoyama, M., Mishima, K., Saito, I., Okano, H., and Mizushima, N. (2006) *Nature* **441**, 885–889
17. Komatsu, M., Waguri, S., Ueno, T., Iwata, J., Murata, S., Tanida, I., Ezaki, J., Mizushima, N., Ohsumi, Y., Uchiyama, Y., Kominami, E., Tanaka, K., and Chiba, T. (2005) *J. Cell Biol.* **169**, 425–434
18. Ravikumar, B., Duden, R., and Rubinsztein, D. C. (2002) *Hum. Mol. Genet.* **11**, 1107–1117
19. Urushitani, M., Kurisu, J., Tsukita, K., and Takahashi, R. (2002) *J. Neurochem.* **83**, 1030–1042
20. Kabuta, T., Hakuno, F., Asano, T., and Takahashi, S. (2002) *J. Biol. Chem.* **277**, 6846–6851
21. Lee, D. H., and Goldberg, A. L. (1998) *Trends Cell Biol.* **8**, 397–403
22. Ostrowska, H., Wojcik, C., Wilk, S., Omura, S., Kozlowski, L., Stoklosa, T., Worowski, K., and Radziwon, P. (2000) *Int. J. Biochem. Cell Biol.* **32**, 747–757
23. Meng, L., Mohan, R., Kwok, B. H., Elofsson, M., Sin, N., and Crews, C. M. (1999) *Proc. Natl. Acad. Sci. U. S. A.* **96**, 10403–10408
24. Garcia-Echeverria, C. (2002) *Mini Rev. Med. Chem.* **2**, 247–259
25. Qin, Z. H., Wang, Y., Kegel, K. B., Kazantsev, A., Apostol, B. L., Thompson, L. M., Yoder, J., Aronin, N., and DiFiglia, M. (2003) *Hum. Mol. Genet.* **12**, 3231–3244
26. Cuervo, A. M., Stefanis, L., Fredenburg, R., Lansbury, P. T., and Sulzer, D. (2004) *Science* **305**, 1292–1295
27. Kabeya, Y., Mizushima, N., Ueno, T., Yamamoto, A., Kirisako, T., Noda, T., Kominami, E., Ohsumi, Y., and Yoshimori, T. (2000) *EMBO J.* **19**, 5720–5728
28. Webb, J. L., Ravikumar, B., Atkins, J., Skepper, J. N., and Rubinsztein, D. C. (2003) *J. Biol. Chem.* **278**, 25009–25013
29. Blommaart, E. F., Luiken, J. J., Blommaart, P. J., van Woerkom, G. M., and Meijer, A. J. (1995) *J. Biol. Chem.* **270**, 2320–2326
30. Gutierrez, M. G., Master, S. S., Singh, S. B., Taylor, G. A., Colombo, M. I., and Deretic, V. (2004) *Cell* **119**, 753–766
31. Liang, X. H., Jackson, S., Seaman, M., Brown, K., Kempkes, B., Hibshoosh, H., and Levine, B. (1999) *Nature* **402**, 672–676
32. Shimizu, S., Kanaseki, T., Mizushima, N., Mizuta, T., Arakawa-Kobayashi, S., Thompson, C. B., and Tsujimoto, Y. (2004) *Nat. Cell Biol.* **6**, 1221–1228
33. Aquilano, K., Rotilio, G., and Ciriolo, M. R. (2003) *J. Neurochem.* **85**, 1324–1335
34. Kato, S., Takikawa, M., Nakashima, K., Hirano, A., Cleveland, D. W., Kusaka, H., Shibata, N., Kato, M., Nakano, I., and Ohama, E. (2000) *Amyotroph. Lateral Scler. Other Motor Neuron Disord.* **1**, 163–184
35. Bruijn, L. I., Becher, M. W., Lee, M. K., Anderson, K. L., Jenkins, N. A., Copeland, N. G., Sisodia, S. S., Rothstein, J. D., Borchelt, D. R., Price, D. L., and Cleveland, D. W. (1997) *Neuron* **18**, 327–338
36. Matsumoto, G., Stojanovic, A., Holmberg, C. I., Kim, S., and Morimoto, R. I. (2005) *J. Cell Biol.* **171**, 75–85
37. Lee, J. P., Gerin, C., Bindokas, V. P., Miller, R., Ghadge, G., and Roos, R. P. (2002) *J. Neurochem.* **82**, 1229–1238
38. Rabouille, C., Strous, G. J., Crapo, J. D., Geuze, H. J., and Slot, J. W. (1993) *J. Cell Biol.* **120**, 897–908
39. Pramatarova, A., Laganiere, J., Roussel, J., Brisebois, K., and Rouleau, G. A. (2001) *J. Neurosci.* **21**, 3369–3374
40. Lino, M. M., Schneider, C., and Caroni, P. (2002) *J. Neurosci.* **22**, 4825–4832
41. Clement, A. M., Nguyen, M. D., Roberts, E. A., Garcia, M. L., Boillee, S., Rule, M., McMahon, A. P., Doucette, W., Siwek, D., Ferrante, R. J., Brown, R. H., Jr., Julien, J. P., Goldstein, L. S., and Cleveland, D. W. (2003) *Science* **302**, 113–117
42. Urushitani, M., Sik, A., Sakurai, T., Nukina, N., Takahashi, R., and Julien, J. P. (2006) *Nat. Neurosci.* **9**, 108–118
43. Arrasate, M., Mitra, S., Schweitzer, E. S., Segal, M. R., and Finkbeiner, S. (2004) *Nature* **431**, 805–810
44. Saudou, F., Finkbeiner, S., Devys, D., and Greenberg, M. E. (1998) *Cell* **95**, 55–66
45. Schaffar, G., Breuer, P., Boteva, R., Behrends, C., Tzvetkov, N., Strippel, N., Sakahira, H., Siegers, K., Hayer-Hartl, M., and Hartl, F. U. (2004) *Mol. Cell.* **15**, 95–105
46. Nucifora, F. C., Jr., Sasaki, M., Peters, M. F., Huang, H., Cooper, J. K., Yamada, M., Takahashi, H., Tsuji, S., Troncoso, J., Dawson, V. L., Dawson, T. M., and Ross, C. A. (2001) *Science* **291**, 2423–2428

Available online at www.sciencedirect.com
ScienceDirect
ELSEVIER
Biochemical and Biophysical Research Communications 356 (2007) 993–997
BBRC
www.elsevier.com/locate/ybbrc

Evolution of mitochondrial cell death pathway: Proapoptotic role of HtrA2/Omi in *Drosophila*

Tatsushi Igaki [a,1], Yasuyuki Suzuki [b,1], Naoko Tokushige [c], Hiroka Aonuma [d,f], Ryosuke Takahashi [e,*], Masayuki Miura [f,*]

[a] *Department of Genetics, Yale University School of Medicine, Boyer Center for Molecular Medicine, 295 Congress Avenue, New Haven, CT 06536, USA*
[b] *Department of Degenerative Neurological Diseases, National Institute of Neuroscience, National Center of Neurology and Psychiatry, Kodaira, Tokyo 187-8502, Japan*
[c] *Laboratory for Developmental Neurobiology, Brain Science Institute, RIKEN, 2-1 Hirosawa, Wako, Saitama 351-0198, Japan*
[d] *Laboratories for Integrated Biology, Graduate School of Frontier Biosciences, Osaka University, 1-3 Yamadaoka, Suita, Osaka 565-0871, Japan*
[e] *Department of Neurology, Kyoto University Graduate School of Medicine, 54 Shogoin-Kawaharacho, Sakyoku, Kyoto 606-8507, Japan*
[f] *Department of Genetics, Graduate School of Pharmaceutical Sciences, University of Tokyo, 7-3-1 Hongo, Bunkyo-ku, Tokyo 113-0033, Japan*

Received 14 March 2007
Available online 26 March 2007

Abstract

Despite the essential role of mitochondria in a variety of mammalian cell death processes, the involvement of mitochondrial pathway in *Drosophila* cell death has remained unclear. To address this, we cloned and characterized DmHtrA2, a *Drosophila* homolog of a mitochondrial serine protease HtrA2/Omi. We show that DmHtrA2 normally resides in mitochondria and is up-regulated by UV-irradiation. Upon receipt of apoptotic stimuli, DmHtrA2 is translocated to extramitochondrial compartment; however, unlike its mammalian counterpart, the extramitochondrial DmHtrA2 does not diffuse throughout the cytosol but stays near the mitochondria. RNAi-mediated knock-down of DmHtrA2 in larvae or adult flies results in a resistance to stress stimuli. DmHtrA2 specifically cleaves *Drosophila* inhibitor-of-apoptosis protein 1 (DIAP1), a cellular caspase inhibitor, and induces cell death both *in vitro* and *in vivo* as potent as other fly cell death proteins. Our observations suggest that DmHtrA2 promotes cell death through a cleavage of DIAP1 in the vicinity of mitochondria, which may represent a prototype of mitochondrial cell death pathway in evolution.

Keywords: Apoptosis; Cell death; *Drosophila*; HtrA2/Omi; Mitochondria

Mitochondria play crucial roles in regulating cell death in mammals [1,2]. Upon receipt of apoptotic stimuli, the cell activates caspase protease cascade to execute cell death. The activation of caspases is largely regulated by mitochondrial proteins such as cytochrome *c* (cyt *c*), Smac/DIABLO, and HtrA2/Omi, which are released to cytosol following cell death stimuli [1,2]. cyt *c* directly activates the cytosolic caspase-activating protein Apaf-1, thereby triggering a cascade of caspase activations [1,3]. On the other hand, Smac/DIABLO and HtrA2/Omi indirectly activate caspases by antagonizing inhibitor-of-apoptosis proteins (IAPs), a family of cellular caspase inhibitors [4–7]. HtrA2/Omi, as well as cyt *c*, has also been shown to be important for cell survival, as loss of HtrA2/Omi gene results in a neurodegeneration in mice [8,9].

Despite abundant similarities in cell death mechanisms between vertebrates and flies, the involvement of mitochondria in *Drosophila* cell death machinery has remained unclear. *Drosophila* cell death is largely regulated by three killer proteins Reaper, Hid, and Grim. These proteins are thought to be functional counterparts of mammalian mitochondrial killer proteins Smac/DIABLO and HtrA2/Omi, as they bind to and antagonize IAPs through their

* Corresponding authors.
E-mail addresses: ryosuket@kuhp.kyoto-u.ac.jp (R. Takahashi), miura@mol.f.u-tokyo.ac.jp (M. Miura).
[1] These authors contributed equally to this work.

0006-291X/$ - see front matter © 2007 Elsevier Inc. All rights reserved.
doi:10.1016/j.bbrc.2007.03.079

conserved four-amino-acid sequences called RHG (Reaper, Hid, and Grim) motif or IBM (IAP-Binding Motif) [3,10]. Unlike mammalian counterparts, however, RHG normally reside in the cytoplasm and their activities are regulated either at transcriptional levels or by phosphorylation [11]. The presence of two *Drosophila* Bcl-2 family proteins that localize to mitochondria [12,13] indicates that mitochondrial cell death pathway may also exist in flies [14]. Here, in order to investigate the role of mitochondria in *Drosophila* cell death pathway, we cloned and characterized DmHtrA2, a *Drosophila* homolog of HtrA2/Omi. Our data suggest that DmHtrA2 promotes cell death through a cleavage of *Drosophila* IAP1 (DIAP1) in the vicinity of mitochondria, which may represent a prototype of mitochondrial cell death pathway in evolution.

Materials and methods

Stress resistance. For UV-resistance, third-instar larvae were irradiated with 5 mJ/cm^2 UV and allowed to develop at 25 °C. Paraquat resistance was tested essentially as described [15]. Adult flies (age 10–20 days) were starved for 6 h and transferred to vials containing two 2 cm × 2 cm filter squares wetted with 20 mM paraquat (Sigma) in 5% sucrose solution. Survival was scored at 18 or 24 h after the transfer. The ingestion rate was determined by dye intake by adding 10 mg/ml bromophenol blue instead of paraquat. Fly lysate was analyzed by monitoring the absorbance at 595 nm at 18 h.

Recombinant proteins and cleavage assay. The C-terminally His_6-tagged recombinant human HtrA2 protein (HsHtrA2ΔN133-His_6) was described previously [6]. The N-terminally GST-tagged recombinant DmHtrA2 protein (GST-DmHtrA2ΔN92) was produced in the *Escherichia coli*. The protein was purified by affinity chromatography using Glutathione Sepharose™ 4B (Amersham Bioscience). N-terminally FLAG-tagged DIAP1 or Hop was translated *in vitro* in the presence of [^{35}S]-methionine using a TNT T7 Quick Coupled Transcription/Translation System (Promega). [^{35}S]-labeled proteins were incubated with recombinant HtrA2 proteins (100 nM) in Tris buffer containing 50 mM Tris–HCl (pH 7.5), 150 mM NaCl, and 1 mM DTT for 1 h at 37 °C. The reaction mixtures were subjected to SDS–PAGE and visualized by autoradiography.

Cell death assay. Cell death assay was performed as described previously [12]. In brief, S2 cells were transfected with pUAST-derived expression constructs with a driver plasmid pWAGAL4 (actin promoter-GAL4), together with a reporter plasmid pCaspeR-hs-lacZ that encodes β-galactosidase under the control of the *hsp70* promoter. Twenty-four hours after transfection, the cells were heat-shocked at 37 °C and cultured for another 24 h. The cells were lysed at 48 h and assayed for β-galactosidase activity in a reaction mixture containing *o*-nitrophenyl-β-D-galactopyranoside.

For information regarding cloning, expression constructs, antibodies, cell culture, subcellular fractionation, Western blotting, and fly stocks, see Supplementary information.

Results and discussion

We cloned the DmHtrA2 cDNA (DDBJ/EMBL/GenBank, Accession No. AB112473) from the total RNA of wild-type fly embryo. DmHtrA2 encoded a protein of 422 amino acids with an N-terminal transmembrane (TM) domain, a central trypsin-like serine protease domain, and a C-terminal PDZ domain, as well as an IBM-like (ASKM) sequence that locates adjacent to the TM (Supplemental Fig. 1). RT-PCR analysis revealed that DmHtrA2 mRNA was expressed at all stages of *Drosophila* development (Supplemental Fig. 1).

To investigate the role of DmHtrA2 in cell death, we induced cell death in *Drosophila* S2 cells by UV-irradiation. Four hours after irradiation, the cells began to exhibit apoptotic morphological changes (Fig. 1A and B). We found that the protein level of DmHtrA2 was significantly up-regulated in the irradiated cells in a time-dependent

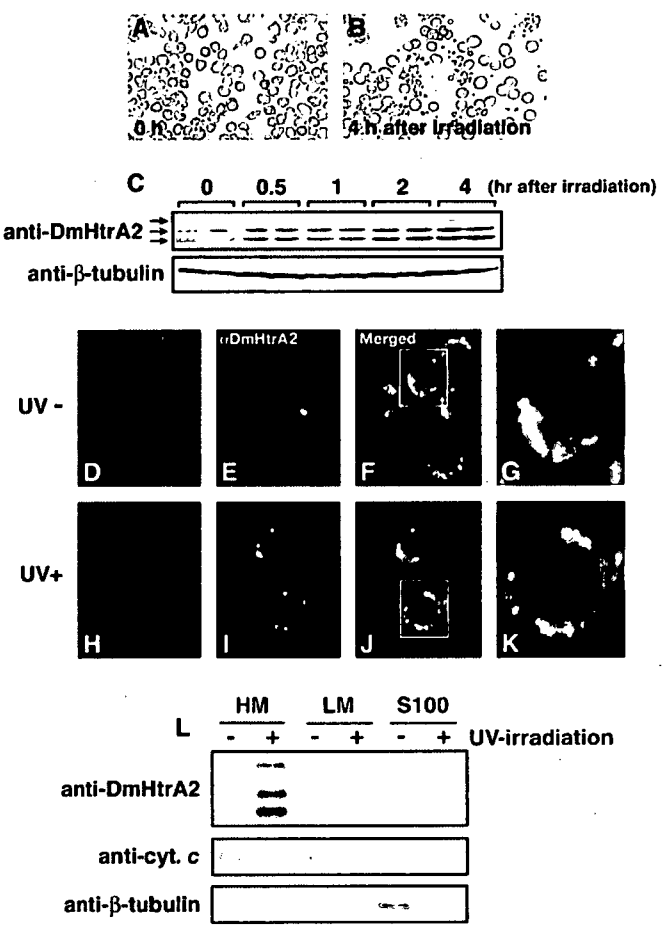

Fig. 1. Apoptotic stimulus up-regulates DmHtrA2 and induces its translocation from mitochondria to extramitochondrial compartment. (A,B) S2 cells were irradiated with UV (200 mJ/cm^2) and cultured for another 4 h. (C) Endogenous DmHtrA2 levels were assessed by Western blotting using an anti-DmHtrA2 antibody before and after UV-irradiation. An anti-β-tubulin antibody was used for a loading control. The anti-DmHtrA2 antibody recognized three bands; the highest band corresponded to the size of full-length form, and the lowest band corresponded to the size of putative mitochondrial mature (ΔN) form (C, upper panel). The experiments were performed using duplicate dishes and were repeated three times. (D–K) Confocal images of S2 cells co-stained with Mitotracker (magenta) and an anti-DmHtrA2 antibody (green). Mitochondria and the endogenous DmHtrA2 protein were visualized before (D–G) or 4 h after (H–K) UV-irradiation (200 mJ/cm^2). G and K show magnified images from F and J, respectively. (L) S2 cells were fractionated before (−) or 4 h after (+) UV-irradiation (200 mJ/cm^2), and the cell lysate was subjected to Western blot analysis using anti-DmHtrA2, anti-cytochrome *c*, and anti-β-tubulin antibodies. For DmHtrA2 protein, the total amount of protein from each fraction was adjusted to 2.5 μg. For cytochrome *c* and β-tubulin, the mitochondrial and cytosolic markers, respectively, an equal volume (10 μl) from each fraction was used for Western analysis.

manner (Fig. 1C). This up-regulation was observed even at 2 h after irradiation, preceding the morphological changes (Fig. 1C). Immunostaining of DmHtrA2 revealed that it exclusively localized to mitochondria under the normal condition (Fig. 1D–G). Four hours after UV-irradiation, the anti-DmHtrA2 staining still showed a punctate pattern with a higher signal intensity, but it no longer merged with the Mitotracker-labeled mitochondria (Fig. 1H–K). This suggests that DmHtrA2 is translocated to extramitochondrial conpartment in response to UV-irradiation. We further analyzed the subcellular localization of DmHtrA2 by fractionating S2 cell lysates before and after irradiation. DmHtrA2 protein was detected in the heavy membrane (HM) fraction, as was cyt *c*, but not in either the light membrane (LM) or cytosolic (S100) fraction (Fig. 1L). We found that UV-irradiation did not alter this distribution (Fig. 1L), suggesting that DmHtrA2 is released to the extramitochondrial compartment but stays in the vicinity of the mitochondria. Since no difference was observed in the mitochondrial membrane potential between control and UV-irradiated S2 cells (Fig. 1D and H; [16]), it is unlikely that the complementary staining of anti-DmHtrA2 and Mitotracker in irradiated cells was due to a loss of membrane potential in a subset of mitochondria.

To examine the physiological role of DmHtrA2, we generated DmHtrA2 knock-down flies using an RNAi construct of DmHtrA2 and a ubiquitous driver da-GAL4. In the knock-down larvae and adults, DmHtrA2 protein level was greatly reduced (Fig. 2A). The knock-down flies were viable and fertile with no detectable morphological abnormalities. We found that the DmHtrA2 knock-down larvae were more resistant to UV-induced lethality compared to control larvae (Fig. 2B). Furthermore, the DmHtrA2 knock-down adult flies were more resistant to dietary paraquat, a superoxide stress agent (Fig. 2C). The ingestion rate of the knock-down flies was not affected (data not shown). These observations suggest that DmHtrA2 is involved in stress-induced toxicity *in vivo*.

Mammalian HtrA2/Omi induces cell death by cleaving and thereby inactivating IAPs through its serine protease activity [4–7]. We therefore assumed that the stress-induced toxicity mediated by DmHtrA2 is through a cleavage of DIAP1. We performed an *in vitro* cleavage assay using recombinant DmHtrA2 and DIAP1 proteins, and found that both *Drosophila* and human HtrA2 proteins specifically cleaved DIAP1 (Fig. 3A). These HtrA2 proteins did not cleave a control protein FLAG-tagged Hop (Hsp70/Hsp90-organizing protein) (Fig. 3A). Thus, the specific serine protease activity of HtrA2/Omi is conserved in *Drosophila*.

Finally, we examined whether DmHtrA2 can kill the cell. Overexpression of DmHtrA2 in S2 cells significantly reduced their viability as potent as other *Drosophila* killer proteins such as Reaper (Fig. 3B and data not shown). This cell death could not be blocked by caspase inhibitors such as DIAP1, p35, or p49, similar to the one caused by human HtrA2/Omi [4,6]. We further examined the toxicity of DmHtrA2 *in vivo*. Overexpression of DmHtrA2 in developing *Drosophila* eye resulted in "no eye" phenotype (Fig. 3C), suggestive of an extensive cell death during development. This phenotype was also resistant to caspase inhibitors (Fig. 3C). Together, these data suggest that DmHtrA2 potently induces cell death through a cleavage of DIAP1.

Our observations suggest that stress stimuli such as UV-irradiation cause translocation of DmHtrA2 from mito-

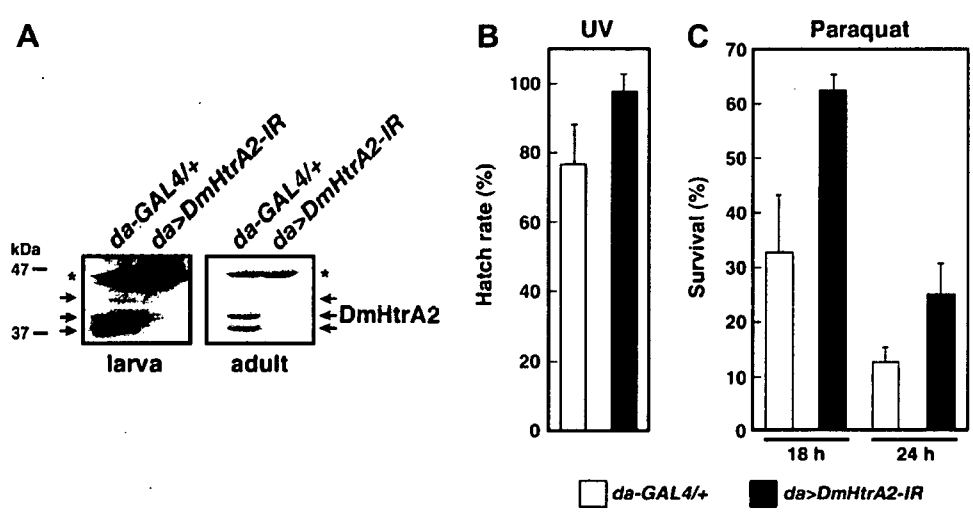

Fig. 2. DmHtrA2 mediates stress stimuli *in vivo*. (A) An RNAi construct (inverted-repeat; IR) for DmHtrA2 (UAS-DmHtrA2-IR) was driven by ubiquitous expression driver da-GAL4 in third-instar larvae or adult flies. Eight animals were homogenized with 96 μl of conventional SDS loading buffer and subjected to SDS–PAGE (4 μl/lane) followed by an anti-DmHtrA2 blotting. The non-specific bands detected by the anti-DmHtrA2 antibody (asterisks) show equal loadings of the protein. (B) Control (da-GAL4) or knock-down (da-GAL4, UAS-DmHtrA2-IR) third-instar larvae were irradiated with UV (5 mJ/cm^2), and the resistance was assessed by the number of adult flies that hatched. (C) Control or knock-down adult flies were starved and subjected to dietary paraquat. Survival was scored at 18 or 24 h after the beginning of ingestion.

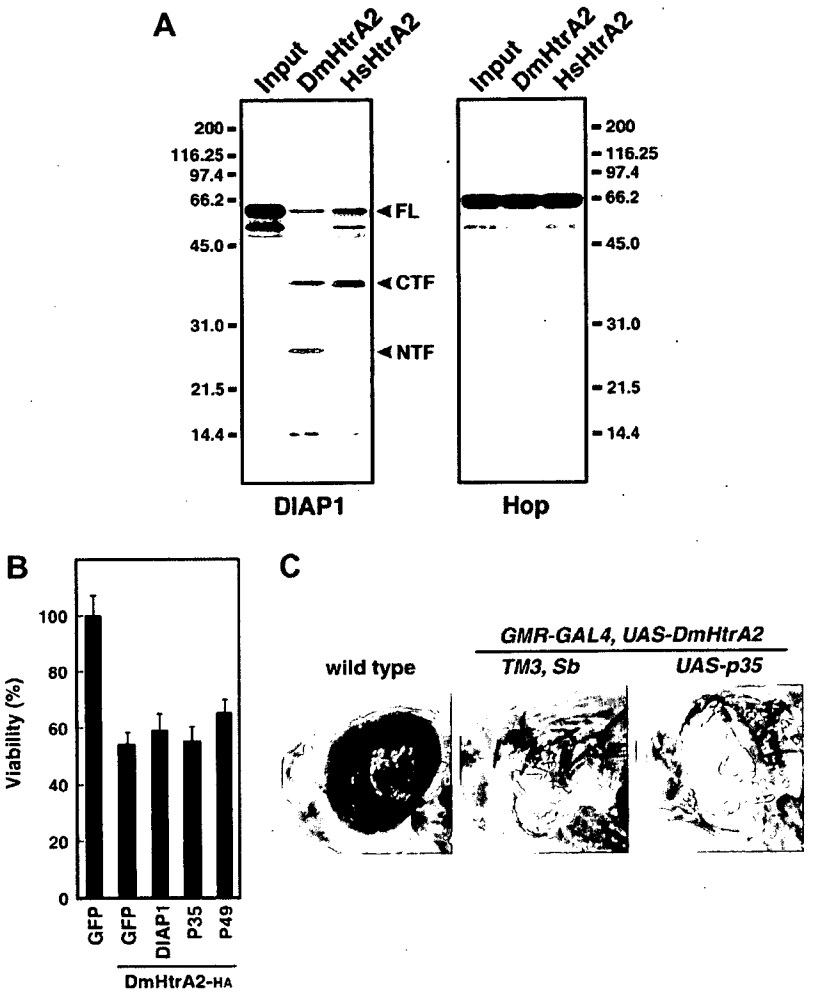

Fig. 3. DmHtrA2 is a potent cell death inducer that cleaves DIAP1. (A) [^{35}S]-labeled DIAP1 or Hop was incubated with *Drosophila* or human HtrA2 recombinant protein, subjected to SDS–PAGE, and visualized by autoradiography. The bands of C-terminal fragment (CTF) and N-terminal fragment (NTF) were predicted by Western blotting of S2 cell lysate co-expressing DmHtrA2 and FLAG-tagged DIAP1 (data not shown). (B) S2 cells were transfected with expression constructs for the indicated proteins and subjected to Cell Death assay. (C) DmHtrA2 was overexpressed in developing *Drosophila* eye using the GMR-GAL4 driver. The eyes at late pupal stage of wild-type, GMR-GAL4/UAS-DmHtrA2$^{2\ 6}$; *TM3, Sb*/+, and GMR-GAL4/UAS-DmHtrA2$^{2\ 6}$; UAS-p35/+ are shown.

chondria to extramitochondrial compartment, which in turn promotes cell death through inactivation of DIAP1. Indeed, a significant proportion of the *Drosophila* caspase DRONC, a fly counterpart of caspase-9, has been shown to localize near mitochondria [17]. Intriguingly, overexpression of DmHtrA2 caused caspase-independent cell death both *in vitro* and *in vivo*. This is consistent with the previous report that down-regulation of DIAP1 triggers a caspase activity-independent cell death pathway that is mediated by DRONC [18]. Our findings suggest that the mitochondrial regulation of cell death machinery could be conserved in *Drosophila*, and that the diverse roles of mitochondria in mammalian systems may have been coopted through the evolution of cell death mechanisms.

Acknowledgments

We thank Nanami Senoo-Matsuda, Hiroshi Kanda, and Ryoko Akai for technical support, Bloomington Stock Center for fly stocks, Yasushi Hiromi for the pWAGAL4 plasmid, Christine Hawkins for p49 plasmid, and John Gurdon and Ryusuke Niwa for the pUAS-GFP plasmid. This work was supported in part by grants from the Japanese Ministry of Education, Science, Sports, Culture and Technology (M.M. and R.T.), and was supported in part by RIKEN Bioarchitect Research Grant (M.M.). T.I. was supported by the Japan Society for the Promotion of Science, in part by a fellowship of Yamanouchi Foundation for Research on Metabolic Disorders, and is a recipient of the long-term fellowship from the Human Frontier Science Program. Y.S. was supported by the Special Postdoctoral Researchers Program, RIKEN.

Appendix A. Supplementary data

Supplementary data associated with this article can be found, in the online version, at doi:10.1016/j.bbrc.2007.03.079.

References

[1] X. Wang, The expanding role of mitochondria in apoptosis, Genes. Dev. 15 (2001) 2922–2933.

[2] D.D. Newmeyer, S. Ferguson-Miller, Mitochondria: releasing power for life and unleashing the machineries of death, Cell 112 (2003) 481–490.

[3] X. Saelens, N. Festjens, L. Vande Walle, M. van Gurp, G. van Loo, P. Vandenabeele, Toxic proteins released from mitochondria in cell death, Oncogene 23 (2004) 2861–2874.

[4] R. Hegde, S.M. Srinivasula, Z. Zhang, R. Wassell, R. Mukattash, L. Cilenti, G. DuBois, Y. Lazebnik, A.S. Zervos, T. Fernandes-Alnemri, E.S. Alnemri, Identification of Omi/HtrA2 as a mitochondrial apoptotic serine protease that disrupts inhibitor of apoptosis protein-caspase interaction, J. Biol. Chem. 277 (2002) 432–438.

[5] L.M. Martins, I. Iaccarino, T. Tenev, S. Gschmeissner, N.F. Totty, N.R. Lemoine, J. Savopoulos, C.W. Gray, C.L. Creasy, C. Dingwall, J. Downward, The serine protease Omi/HtrA2 regulates apoptosis by binding XIAP through a reaper-like motif, J. Biol. Chem. 277 (2002) 439–444.

[6] Y. Suzuki, Y. Imai, H. Nakayama, K. Takahashi, K. Takio, R. Takahashi, A serine protease, HtrA2, is released from the mitochondria and interacts with XIAP, inducing cell death, Mol. Cell. 8 (2001) 613–621.

[7] A.M. Verhagen, J. Silke, P.G. Ekert, M. Pakusch, H. Kaufmann, L.M. Connolly, C.L. Day, A. Tikoo, R. Burke, C. Wrobel, R.L. Moritz, R.J. Simpson, D.L. Vaux, HtrA2 promotes cell death through its serine protease activity and its ability to antagonize inhibitor of apoptosis proteins, J. Biol. Chem. 277 (2002) 445–454.

[8] J.M. Jones, P. Datta, S.M. Srinivasula, W. Ji, S. Gupta, Z. Zhang, E. Davies, G. Hajnoczky, T.L. Saunders, M.L. Van Keuren, T. Fernandes-Alnemri, M.H. Meisler, E.S. Alnemri, Loss of Omi mitochondrial protease activity causes the neuromuscular disorder of mnd2 mutant mice, Nature 425 (2003) 721–727.

[9] L.M. Martins, A. Morrison, K. Klupsch, V. Fedele, N. Moisoi, P. Teismann, A. Abuin, E. Grau, M. Geppert, G.P. Livi, C.L. Creasy, A. Martin, I. Hargreaves, S.J. Heales, H. Okada, S. Brandner, J.B. Schulz, T. Mak, J. Downward, Neuroprotective role of the Reaper-related serine protease HtrA2/Omi revealed by targeted deletion in mice, Mol. Cell. Biol. 24 (2004) 9848–9862.

[10] L.M. Martins, The serine protease Omi/HtrA2: a second mammalian protein with a Reaper-like function, Cell. Death. Differ. 9 (2002) 699–701.

[11] B.A. Hay, J.R. Huh, M. Guo, The genetics of cell death: approaches, insights and opportunities in Drosophila, Nat. Rev. Genet. 5 (2004) 911–922.

[12] T. Igaki, H. Kanuka, N. Inohara, K. Sawamoto, G. Nunez, H. Okano, M. Miura, Drob-1, a Drosophila member of the Bcl-2/CED-9 family that promotes cell death, Proc. Natl. Acad. Sci. USA 97 (2000) 662–667.

[13] L. Quinn, M. Coombe, K. Mills, T. Daish, P. Colussi, S. Kumar, H. Richardson, Buffy, a Drosophila Bcl-2 protein, has anti-apoptotic and cell cycle inhibitory functions, EMBO J. 22 (2003) 3568–3579.

[14] T. Igaki, M. Miura, Role of Bcl-2 family members in invertebrates, Biochim. Biophys. Acta 1644 (2004) 73–81.

[15] Y.J. Lin, L. Seroude, S. Benzer, Extended life-span and stress resistance in the Drosophila mutant methuselah, Science 282 (1998) 943–946.

[16] K.C. Zimmermann, J.E. Ricci, N.M. Droin, D.R. Green, The role of ARK in stress-induced apoptosis in Drosophila cells, J. Cell. Biol. 156 (2002) 1077–1087.

[17] L. Dorstyn, S. Read, D. Cakouros, J.R. Huh, B.A. Hay, S. Kumar, The role of cytochrome *c* in caspase activation in Drosophila melanogaster cells, J. Cell. Biol. 156 (2002) 1089–1098.

[18] T. Igaki, Y. Yamamoto-Goto, N. Tokushige, H. Kanda, M. Miura, Down-regulation of DIAP1 triggers a novel Drosophila cell death pathway mediated by Dark and DRONC, J. Biol. Chem. 277 (2002) 23103–23106.